Published in final edited form as:
Calcif Tissue Int. 2013 September ; 93(3): 222–232. doi:10.1007/s00223-013-9745-3.

Effects of pH on the Production of Phosphate and Pyrophosphate by Matrix Vesicles' Biomimetics

Ana Maria S. Simão[a,c], **Maytê Bolean**[a], **Marc F. Hoylaerts**[b], **José Luis Millán**[c], and **Pietro Ciancaglini**[a,c,*]

[a]Department of Chemistry, FFCLRP-USP, Ribeirão Preto, SP, Brazil

[b]Center for Molecular and Vascular Biology, University of Leuven, Leuven, Belgium

[c]Sanford Children's Health Research Center, Sanford-Burnham Medical Research Institute, La Jolla, CA, USA

Abstract

During endochondral bone formation, chondrocytes and osteoblasts synthesize and mineralize the extracellular matrix through a process that initiates within matrix vesicles (MVs) and ends with bone mineral propagation onto the collagenous scaffold. pH gradients have been identified in the growth plate of long bones, but how pH changes affect the initiation of skeletal mineralization is not known. Tissue-nonspecific alkaline phosphatase (TNAP) degrades extracellular inorganic pyrophosphate (ePP_i), a mineralization inhibitor produced by ectonucleotide pyrophosphatase/phosphodiesterase-1 (NPP1), while contributing P_i from ATP to initiate mineralization. TNAP and NPP1, alone or combined, were reconstituted in dipalmitoylphosphatidylcholine (DPPC) liposomes to mimic the microenvironment of MVs. The hydrolysis of ATP, ADP, AMP and PP_i was studied at pH 8 and 9 and compared to the data determined at pH 7.4. While catalytic efficiencies in general were higher at alkaline pH, PP_i hydrolysis was maximal at pH 8 and indicated a preferential utilization of PP_i over ATP, at pH 8 versus 9. In addition, all proteoliposomes induced mineral formation when incubated in a synthetic cartilage lymph (SCL) containing 1 mM ATP as substrate and amorphous calcium phosphate (ACP) or calciumphosphate- phosphatidylserine complexes (PS-CPLX) as nucleators. Propagation of mineralization was significantly more efficient at pHs 7.5 and 8 than at pH 9. Since a slight pH elevation from 7.4 to 8 promotes considerably more hydrolysis of ATP, ADP and AMP primarily by TNAP, this small pH change facilitates mineralization, especially via upregulated PP_i hydrolysis by both NPP1 and TNAP, further elevating the P_i/PP_i ratio, thus enhancing bone mineralization.

Keywords

biomineralization; alkaline pH; microenvironment; proteoliposomes; pyrophosphate; ATP

During endochondral bone formation, chondrocytes and osteoblasts synthesize and mineralize the extracellular matrix [1] through a process that starts within matrix vesicles (MVs) as the sites of initiation of hydroxyapatite (HA) deposition and ends with bone mineral propagation onto the collagenous scaffold. The phosphatases tissue-nonspecific alkaline phosphatase (TNAP, EC 3.1.3.1) and ectonucleotide pyrophosphatase/

*Corresponding author. Department of Chemistry, FFCLRP-USP, Av. Bandeirantes, 3900, 14040-901, Ribeirão Preto, SP, Brazil. Tel.: +55 16 3602-3753; Fax: +55 16 3602-4838; pietro@ffclrp.usp.br.

phosphodiesterase-1 (NPP1, EC 3.6.1.9) have been implicated in MV-mediated calcification [2].

TNAP is confined to the cell surface of osteoblasts and chondrocytes, including the membranes of their shed MVs [3]. Several studies have proposed a phosphate-generating function for TNAP producing inorganic phosphate (P_i) needed for HA crystallization [4], while others proposed that TNAP's role is to hydrolyze the mineralization inhibitor PP_i [5] to facilitate mineral precipitation and growth [6], a conclusion supported by our own work [7,8]. Hence, by hydrolyzing extracellular PP_i, a proper concentration of this mineralization inhibitor is maintained to allow normal bone mineralization.

PP_i is generated by the ectonucleotide pyrophosphatase/phosphodiesterase (NPP) family of isozymes. NPP1 is plasma membrane-bound, whereas autotaxin (NPP2) is secreted and B10 (NPP3) is abundant in intracellular spaces [9]. All three isozymes are expressed in a wide variety of tissues, including bone and cartilage [10], and they have the common ability to hydrolyze diesters of phosphoric acid into phosphomonoesters. NPP1 is highly abundant on the surfaces of osteoblasts and chondrocytes as well as on the membrane of their MVs and it has a role in inhibiting HA precipitation by its PP_igenerating property [11]. However, NPP1 can also act as a phosphatase [12], and we have shown that it can generate P_i from both ATP and PP_i in the MV microenvironment [13,14].

Initiation of biomineralization occurs in a microenvironment which determines the biological properties and physiological interplay between MV-associated enzymes and proteins. Recent data [15] suggest that the location of TNAP on the membrane of MVs plays a role in determining substrate selectivity in this microcompartment, suggesting that assays of TNAP bound to MVs or to liposome systems might be more relevant than assays done with solubilized enzymes, particularly when studying the hydrolysis of organophosphate substrates. The ability of synthetic or natural vesicles [16,17] to mimic the structure and function of biomembranes makes these structures an advantageous and convenient model to help us advance our understanding of MV-mediated calcification. Simão et al. [14] reconstituted either TNAP, NPP1 or both together into liposome membranes and evaluated their synergistic and/or antagonistic activity, at physiological pH, when presented with physiological substrates relevant to the biomineralization process.

In addition to biophysical factors, it has been shown that also the pH may play a regulatory role during the mineralization process [18–20]. Since the hydrolysis of ATP, ADP, AMP and PP_i by TNAP and NPP1 critically contributes to bone formation and since these enzymes show an alkaline pH optimum [14,21,22], we have studied the hydrolysis of these phosphosubstrates by proteoliposomes harboring TNAP and/or NPP1 at slightly alkaline pH (pH 8 vs. 9) and compared our findings with data obtained at physiological pH. Our results show that even modest pH elevations have a strong impact on the phosphosubstrates hydrolysis rate.

Previous studies discovered a nucleational core that drives mineral formation by native MVs [23,24]. Components identified to be essential were amorphous calcium phosphate (ACP) and its combined form with phosphatidylserine (PS), the calcium-phosphate-lipid complexes (PS-CPLX). Here we have also examined the effects of ACP and PS-CPLX for their ability to modulate mineral formation induced by proteoliposomes containing either TNAP, NPP1 or both together when incubated in a synthetic cartilage lymph (SCL) carefully constructed to contain physiological levels of electrolytes and substrates.

Materials and Methods

Cell Culture and Preparation of Membrane Fractions Rich in TNAP and NPP1

Cells were prepared and cultured according to Simão et al. [25]. A plasmid containing rat NPP2 Nterminal signal peptide (33 residues) connected to the residues of mouse NPP1 (residues 85–905) was kindly provided by Dr. Bollen [26]. A glycosylphosphatidylinositol (GPI)-anchored form of mouse NPP1 was produced and expressed as described [14]. Membrane-bound TNAP and NPP1 were obtained from 14-day primary osteoblast cultures or from transfected COS-1 cells, respectively, as described [14].

Solubilization and Partial Purification of GPI-anchored Enzymes with Polyoxyethylene-9-Lauryl Ether (Polidocanol)

Membrane-bound enzymes (0.2 mg/ml total protein) were solubilized with 1% polidocanol (w/v) (final concentration) for 2 h, with constant stirring, at 25 °C. After centrifugation at 100,000×g for 1 h at 4 °C, detergent-free solubilized enzymes were obtained using 200 mg of Calbiosorb resin and 1 ml of polidocanol-solubilized enzyme (~0.03 mg of protein/ml), as previously described [27]. All protein concentrations were estimated in the presence of 2% (w/v) SDS [28]. Bovine serum albumin was used as a standard.

Liposome Preparation and Incorporation of GPI-anchored TNAP and NPP1 into Liposomes

Dipalmitoyl phosphatidylcholine (DPPC) liposomes and DPPC proteoliposomes containing TNAP, NPP1 or TNAP + NPP1 were prepared as previously described [14].

Enzymatic Assays

For ATP, ADP, AMP, and PP_i hydrolysis, the phosphomonohydrolase activities were assayed discontinuously, at 37 °C, by measuring the amount of inorganic phosphate liberated, as before [29], adjusting the assay medium to a final volume of 0.5 ml. The reaction was initiated by the addition of the enzyme and stopped with cold 30% trichloracetic acid (TCA) at appropriate time intervals. The reaction mixture was centrifuged at 4000×g, and phosphate was quantified in the supernatant according to the procedure described by Heinonen and Lahti [30]. Standard assay conditions were 50 mM 2-amino-2-methyl-propan-1-ol (AMPOL) buffer, pH 9, containing 2 mM $MgCl_2$ and substrate, or 50 mM Tris-HCl buffer, pH 8, containing 2 mM $MgCl_2$ and substrate. Initial velocities were constant for at least 90 min, provided that less than 5% of substrate was hydrolyzed. Controls without added enzyme were included in each experiment to correct for non-enzymatic hydrolysis of substrate. One enzyme unit (1 unit/mg) is defined as the amount of enzyme hydrolyzing 1.0 nmol of substrate/min/mg of protein. Maximum velocity (V_{max}), apparent dissociation constant ($K_{0.5}$), and Hill coefficient (n) obtained from substrate hydrolysis were calculated as described [31]. Data were reported as the mean of triplicate measurements of three different enzyme preparations. Statistically significant differences were defined as $p \leq 0.05$.

Measurement of Nucleotide Hydrolysis by HPLC

Hydrolysis of ATP and ADP by proteoliposomes was determined at 37 °C in 50 mM AMPOL buffer, pH 9, containing 2 mM $MgCl_2$ and substrate. Reactions were started by the addition of enzyme and, at predetermined intervals, samples were removed and immediately quantified. Nucleotides were separated and quantified by HPLC, injecting a 20-μl aliquot of the sample into a C_{18} reversed-phase column (Shimadzu) and eluting it at 1.5 ml/min, with the mobile phase consisting of 50 mM potassium-phosphate buffer (pH 6.4), 5 mM tetrabutylammonium hydrogen sulfate and 18% (v/v) methanol. A_{260nm} was continuously

monitored and nucleotide concentrations were determined from the area under the absorbance peaks [14].

Synthesis of ACP and PS-CPLX

The synthesis of ACP and PS-CPLX was done according to the method described by Genge et al. [32]. An emulsion of PS was prepared by drying 1.25 mg of PS in chloroform under N_2 to form a thin film in a test tube. Then 2 ml of the P_i-rich intracellular phosphate (ICP) buffer was added. This buffer, which modeled the electrolyte composition of ultrafiltrates of the intracellular fluid of growth plate chondrocytes [33], contained 106.7 mM K^+, 45.1 mM Na^+, 1.5 mM Mg^{2+}, 115.7 mM Cl^-, 23.0 mM P_i, 10 mM HCO_3^-, 1.5 mM $SO^{4\,2-}$, and 3.1 mM N_3- as a preservative; its total molarity was 153.3 mM, and its pH was 7.2. The tube was sonicated for 2 min at 25 °C to form a uniform translucent emulsion of small unilamellar vesicles. For example, to make the nucleators, 17.5 μl of 100 mM $CaCl_2$ was added to 1 ml of the PS emulsion with rapid stirring. On the addition of Ca^{2+} to ICP buffer, ACP instantly forms because of the high $Ca^{2+}\times P_i$ ion product, and during this formative period, nascent ACP combines with the PS liposomes to form the insoluble PS-CPLX, which is then harvested by centrifugation for 5 min at approximately 15,000×g. The pellets were resuspended in 1 ml of 16.5 mM Tris buffer, pH 8 by brief sonication to yield uniform suspensions. In some experiments, PS was omitted and the 100 mM $CaCl_2$ stock was added into the ICP buffer with rapid stirring to form ICP-based ACP. These procedures model the processes that occur in growth plate chondrocytes, where intracellular Ca^{2+} levels increase dramatically at sites of MV formation [34].

Microplate Mineralization Assay with Proteoliposomes

TNAP-, NPP1-, and TNAP plus NPP1-proteoliposomes were incubated in SCL containing ACP or PS-CPLX, at three different pHs (7.5, 8 and 9). SCL contained 2 mM Ca^{2+} and 1 mM ATP as the P_i source, in addition to 104.5 mM Na^+, 133.5 mM Cl^-, 63.5 mM sucrose, 16.5 mM Tris, 12.7 mM K^+, 5.55 mM glucose, 1.83 mM HCO_3^-, and 0.57 mM Mg sulfate [35]. Empty liposomes without incorporated enzymes were used as control. Mineral formation was measured by turbidity (i.e., absorbance) at 340 nm (A_{340nm}) using a multiwell microplate assay system described by Genge and coworkers [36]. Triplicate samples (100 μl) of each were successively distributed into wells of a 96-well microplate. Turbidity measurements were made after brief (10 s) agitation, after 48 h of incubation at 37°C, using a Molecular Devices M3 microplate reader. All measurements were performed in triplicate. Statistical comparisons were done by one-way ANOVA followed by Tukey's test. P values less than 0.05 are considered significant.

Results

Since the optimum pH for the activity of TNAP and NPP1 is alkaline [14,21,22], we have compared the effects of slightly alkaline pH (pH 8 vs. 9) with those obtained at physiological pH [14] on the hydrolysis of the physiological substrates ATP, ADP, AMP and PP_i by proteoliposomes harboring TNAP alone, NPP1 alone or both together. Table 1 and Table 2 summarize the kinetic parameters obtained at pH 8 and 9, respectively. Fig. 1 and Fig. 2 illustrate how the activities depend on substrate concentration, at pH 8 and 9, respectively.

The highest hydrolysis rate (V_m) for TNAP- and for NPP1-proteoliposomes was found for AMP at pH 9 and for PP_i at pH 8, respectively. At pH 9, similarly to what happens at pH 7.4 [14], the $K_{0.5}$ values were quite different (Table 2). The catalytic efficiencies ($k_{cat}/K_{0.5}$) were also lower for NPP1-proteoliposomes compared with TNAP-proteoliposomes for all substrates at both pHs, pointing to a major role of TNAP in the hydrolysis of these substrates

(Tables 1 and 2). Hence, the activity patterns of TNAP-, NPP1-, and TNAP + NPP1-proteoliposomes at alkaline pHs suggested a predominant activity of TNAP in mixed vesicles when compared with NPP1. The catalytic efficiencies at pH 9 were only higher for the hydrolysis of AMP, largely due to the lower $K_{0.5}$ at this pH (Table 2). The catalytic efficiencies of ATP, ADP and PP_i hydrolysis by NPP1 were considerably higher at pH 8 (Table 1).

When the hydrolysis rates, affinities and catalytic efficiencies were reported relative to the corresponding values at physiological pH (Table 3), we could calculate a pH 8/pH 7.4 and pH 9/pH 7.4 ratio for each parameter, allowing normalized efficiency comparisons, relative to the previously determined values [14]. Affinity constants were minimally affected from pH 7.4 to pH 8, but increased considerably when the pH was increased to pH 9 (Table 3). Despite relative higher hydrolysis rates (V_m) at pH 9 compared to pH 8, the catalytic efficiencies were considerably higher at pH 8, relative to the values at pH 7.4. Catalysis was non-cooperative during ATP hydrolysis at both alkaline pHs by all proteoliposomes (Tables 1 and 2), in contrast to the positive cooperativities observed at physiologic pH [14].

Hydrolysis of PP_i showed no cooperative regulation at pH 9, but positive cooperativity was observed at pH 8 for proteoliposomes harboring NPP1 (Tables 1 and 2). $K_{0.5}$ values were quite similar at alkaline pHs (Tables 1 and 2), but higher than the values at pH 7.4 [14]. Surprisingly, an increase in the hydrolysis rates and catalytic efficiencies was observed for NPP1-proteoliposomes at pH 8, compared to pH 7.4 [14] (Table 3).

Thus, comparing the differences in the kinetic parameters obtained for the different substrates (Tables 1, 2 and 3), we observed that the hydrolysis rates (V_m) increase significantly at alkaline pHs for both enzymes and their combination, but since the affinities ($K_{0.5}$) hardly changes and the catalytic efficiencies ($k_{cat}/K_{0.5}$) are much higher for PP_i when compared with ATP, ADP and AMP, a small pH elevation to pH 8 induces a relative advantage for PP_i hydrolysis by NPP1 over phosphonucleotides hydrolysis, an advantage less clear at pH 9 (Table 3). Hence, these experiments illustrate that a small elevation in the pH considerably influences enzyme catalysis by TNAP and NPP1 differently, speeding up PP*i* hydrolysis, resulting in an elevation of the P*i*/PP*i* ratio.

Because our data suggested a balanced hydrolysis for the various substrates, we also investigated the nucleotide hydrolysis at pH 9, monitoring the formation of reaction intermediates as a function of time during hydrolysis of ATP and ADP, separating and quantifying the products by HPLC. The amounts of ADP, AMP and/or adenosine produced for the different proteoliposomes are shown for the hydrolysis of ATP (Fig. 3) and ADP (Fig. 4).

Hydrolysis of ATP resulted in ADP, AMP and adenosine formation by the various proteoliposomes with different efficiencies, as predicted by Table 2 (Fig. 3). Nonetheless, the time-dependent catalysis of ATP is more pronounced in TNAP-proteoliposomes than in the liposomes containing NPP1, confirming the major role of TNAP in the hydrolysis of this substrate. In accordance with the predominant role of TNAP in the TNAP-proteoliposomes, the concentration of the reaction intermediate ADP was higher for TNAP- and TNAP + NPP1-proteoliposomes (Fig. 3a). AMP only accumulated to low levels because it was hydrolyzed with high catalytic efficiency to adenosine and phosphate (Table 2). Adenosine accumulated to a higher degree upon incubations with TNAP- and TNAP + NPP1-proteoliposomes (Fig. 3c). The larger adenosine accumulation by these proteoliposomes reflects the higher activity of TNAP during ADP formation and its further breakdown to AMP and adenosine compared with NPP1, which generates AMP and PP*i* directly, in addition to behaving as a phosphatase (Table 2 and Fig. 5).

When ADP was used, the highest catalysis rate was observed (Fig. 4) again for TNAP-proteoliposomes. However, catalysis of ADP by NPP1-proteoliposomes (Table 2 and Fig. 4) confirmed that this enzyme can behave as a phosphatase.

Compared to control incubations with empty liposomes, all proteoliposomes induced mineral formation when incubated in SCL containing 1 mM ATP as substrate, but the induction of mineralization was equivalent at pH 7.5 and 8, and considerably less at pH 9 (Fig. 6). When comparing the effects of ACP and PS-CPLX in modulating mineral formation, both complexes did not present significant differences at pHs 7.5 and 8, but at pH 9 PS-CPLX had a more pronounced effect on mineral formation by proteoliposomes containing TNAP when compared to the proteoliposomes containing NPP1 (Fig. 6). Yet, TNAP + NPP1 proteoliposomes triggered significantly more extensive P*i*-dependent mineralization than TNAP proteoliposomes, despite the lower content in the former proteoliposomes [14], suggestive of additive hydrolytic activities for NPP1 and TNAP.

Discussion

Endochondral calcification is a complex process in which Ca^{2+} and P_i in solution are processed and brought together to induce precipitation of a mineral phase that ultimately forms HA, the principal mineral of bone. One of the essential features of mineralization-inducing MVs is the presence of a nucleation core [23,24] composed of ACP, complexed in part with PS to form calcium-phosphate-lipid complexes (PS-CPLX) capable of inducing mineral formation when incubated in a SCL [36,37,38]. It is important to recognize that ACP is a kinetically unstable mineral that forms only when both Ca^{2+} and P_i are present in high (millimolar) levels [39,40]. Thus, the presence of ACP provides important clues to the process of MV formation. Although P_i-containing PS-CPLXs can induce HA formation, *in vivo* many factors appear to be involved in regulating its formation and activity [41]. PS-CPLXs are present at the early stages of almost all calcifying tissues, as growth plate cartilage [42], bone [43], and MVs [44].

One of the most effective ways to destroy the ability of the nucleational core to induce mineral formation is simple exposure to isosmotic, pH 6 citrate buffer [23]. This reveals that it is highly sensitive to even mildly acidic conditions. On the other hand, at pH 8, the nucleational core is highly stable and insoluble. Past studies on the formation of mineral have shown that the nucleational activity of the MVs and the nucleational core is operative only within a very narrow pH range – between 7.4–7.8 [45]. Either below or above this range, its ability to nucleate mineral formation was very reduced. But in the studies reported by Wu et al. [46], the pH range in which rapid mineral formation occurred was broader (pH 7.4– 8.0). This is in agreement with our data, since the induction of mineralization by our proteoliposomes, in the absence of pyrophosphate was more efficient at pHs 7.5 and 8 and already much less at pH 9, although the optimum pH for the activities of TNAP and NPP1 is alkaline. This difference may be due to the fact that substrate hydrolysis occurs in a lipidic microenvironment while the process of nucleation/mineralization takes place in a different microenvironment, thus the optimum pH for substrate hydrolysis may be distinct from the optimum pH for mineralization, which, moreover, depends on the biophysical properties of the calcium-phosphate complexes and their stability, both pH dependent processes [47].

Proteoliposomes can be obtained by mechanical dispersion, sonication, extrusion, solvent dispersion, co-solubilization with detergents, reverse phase evaporation and direct insertion after detergent removal [17,48,49]. Our long term goal is to reconstitute more complex proteoliposomes containing TNAP, NPP1, PHOSPHO1 [50], Pit-1/2, ANK, Annexins, etc. [51], that will recapitulate the key events leading to initiation of MV-mediated calcification

in vitro, since the lipid membrane plays an important role as a nucleation agent in the biomineralization process [52], as a protective and/or activation agent [53].

In order to understand the physiological interplay between important MV-associated enzymes in the initiation of biomineralization, it is important to keep in mind the microenvironment in which these enzymes function, which can have a profound effect on their biological properties, since the lipid membrane plays an important role in the initiation of the biomineralization process [54,55]. Thus, the ability of synthetic or natural vesicles [16,17] to mimic the structure and function of biomembranes makes these structures an advantageous and convenient model to reconstitute either TNAP, NPP1 or both together, since the modulation of enzymes activities by the lipid microenvironment seems to be common between enzymes that have a glycosylphosphatidylinositol (GPI) anchor. Lehto and Sharom [56] reported a reduction in the catalytic efficiency of the enzyme 5'-nucleotidase upon insertion of the protein into liposomes with different lipid composition, and the activity could be restored upon enzyme release from the membranes after treatment of the proteoliposomes with GPI-specific PLC. They reported that the degree of activity reduction was dependent on the lipid bilayer where the GPI anchor was inserted, suggesting that different lipids affect the activity of the enzyme in different ways, maybe through alteration in protein conformation transmitted from the membrane to the protein solely through the GPI anchor [57]. We have previously documented that although the enzymatic efficiency (k_{cat}/K_m) remained comparable between polidocanol-solubilized and membrane-bound TNAP for all substrates used, the value of k_{cat}/K_m for the GPI-specific PLC-solubilized enzyme increased ~ 108-, 56-, and 556-fold for *p*NPP, ATP, and PP_i, respectively, compared with the membrane-bound enzyme [15].

Bone homeostasis is profoundly affected by local pH. The skeleton contains a large reserve of alkaline mineral (hydroxyapatite), which is ultimately available to neutralize metabolic H^+ if acid-base balance is not maintained within narrow limits [20]. Bone cells are extremely sensitive to the direct effects of pH: acidosis inhibits mineral deposition by osteoblasts but activates osteoclasts to resorb bone and other mineralized tissues [20]. These responses act to maximize the availability of OH^- ions from HA in solution, where they can buffer excess H^+. The mechanisms by which bone cells sense pH changes are likely to be complex, involving ion channels and receptors in the cell membrane, and direct intracellular effects [20].

Most of the studies correlating pH with different aspects of the biomineralization process are done at pHs close to physiological pH, although pH appears to play a regulatory role during the mineralization process [18–20]. Wu et al. [19] reported numerous focal elevations in pH (> 8.0) in central regions of the maturing and early hypertrophic chondrocytes, with lower pH (6.5–7.2) near the cell periphery of the late hypertrophic and calcifying cells, suggesting that this pattern of cytoplasmic alkalinization and subsequent acidification contributes to loading of Ca^{2+} and P_i into MVs during their formation by the chondrocytes. Chakkalakal et al. [18] reported that the pH of repair tissue fluids may play a regulatory role in the healing and mineralization of bone, suggesting that the process of mineralization and bone repair is tissue pH-dependent. Even when the formation of HA was investigated in the pH range 9.5–12.0 [58], the influence of mild pH fluctuations on the players implicated in the biomineralization process is less well known.

P_i transport into MVs appears to take place by at least two pathways: the first being mediated by a P_i transporter, *e.g.*, the type-III Na^+-dependent phosphate transporter (NaP_iT) [59], and a second not strictly Na^+-dependent [60]. This second category has been shown to be alkaline pH-specific. So, an alkaline pH would favor mineralization by promoting P_i transport to the inner of MVs. Besides, Balcerzak et al. [61] characterized the proteome of

MVs isolated from chicken embryo bones and cartilage, and reported the presence of H^+-ATPase, making it possible to establish a pH gradient, allowing a more alkaline pH in the neighborhood of this pump.

The hydrolysis rates were quite different at pH 7.4 and alkaline pHs (Table 3), being relatively slower at physiological pH for all substrates. But analysis of $K_{0.5}$ values (Table 3) for pHs 8 and 9 shows that the affinities for PP_i are comparable for the combined enzymes proteoliposomes, such not being the case for ATP. Also, at alkaline pHs, the catalytic efficiencies are much higher for both TNAP- and NPP1-proteoliposomes for PP_i hydrolysis than for ATP hydrolysis. Since at pH 8, NPP1 becomes such an efficient enzyme in catalyzing PP_i, our findings suggest that mild pH elevations will convert PP_i into a preferred substrate, for both TNAP and NPP1. A further elevation of the pH to 9 does not further drive this differentiation, since the catalytic efficiencies for PP_i conversion by NPP1 drop again. Likewise, due to the high $K_{0.5}$ values at pH 9, catalysis of ATP, ADP and AMP does not further improve. Increasing pH also impacts on the solubility of Ca (pyro)phosphate [47], strongly reducing the solubility of calciumphosphate, at pH > 8. This is clearly illustrated in our present study, where poor mineralization occurred at pH 9. In view of the limited solubility of Mg pyrophosphate at physiological pH (around 40 μM), it is not surprising that a gain for the PP_i hydrolysis benefits from a narrow pH range only. Further pH elevation beyond pH 8 will affect the solubility of Ca and Mg pyrophosphate, i.e. will no longer have a beneficial effect on bone mineralization.

Our data and those of others have conclusively demonstrated that a major role of TNAP is to restrict the extracellular pool of PP_i to allow controlled calcification to proceed [7,8]. The ability of TNAP to use ATP as substrate to initiate calcification has also been documented by many investigators [5,62], although the details of how ATP-derived P_i participates in calcification remain to be established. Our own work has confirmed that purified TNAP and MVs efficiently hydrolyze ATP as well as its metabolites ADP and AMP [13]. It is well known that pH plays an important role in determining the behavior of TNAP, and also of NPP1, as a pyrophosphatase or as an ATPase. Our work shows that a slight elevation in pH from 7.4 to 8 significantly increases the hydrolysis of PP_i by NPP1 and the hydrolysis of ATP by TNAP. This implies that small pH fluctuations will facilitate bone formation by elevating the P_i/PP_i ratio at least in the very narrow pH zone where the nucleational core is operative, up to a maximum of pH 8 [45].

The use of proteoliposomes suggests that TNAP activity and specificity in phosphosubstrate hydrolysis can be enhanced by slight local pH elevations in the neighborhood of calcifying MVs, affecting biomineralization. A slightly alkaline pH outside the MVs could favor two mechanisms: provide larger amounts of P_i during nucleation of the first HA crystals and reduce PP_i more efficiently, enough to support crystals growth along collagen fibrils. The critical balance between these reactions (Fig. 5) is believed to establish a proper P_i/PP_i ratio, conductive to biomineralization.

Acknowledgments

We thank Professor Mathieu Bollen (Leuven, Belgium) for providing the NPP2/NPP1 expression construct. This work was supported in part by Fundaçã o de Amparo à Pesquisa do Estado de São Paulo (FAPESP), Coordenação de Aperfeiçoamento de Pessoal de Nível Superior (CAPES), Conselho Nacional de Desenvolvimento Científico e Tecnológico (CNPq) and grants [DE12889], [AR53102] and [AR47908] from the National Institutes of Health (NIH), USA. AMSS was recipient of studentships from CAPES and FAPESP.

References

1. Boskey, A. Dynamics of Bone and Cartilage Metabolism. Seibel; Robins; Biezikian, editors. Academic Press; 2006. p. 201-212.
2. Millán JL. The Role of Phosphatases in the Initiation of Skeletal Mineralization. Calcif Tissue Int. 2012 (in press).
3. Ali SY, Sajdera SW, Anderson HC. Isolation and characterization of calcifying matrix vesicles from epiphyseal cartilage. Proc Natl Acad Sci USA. 1970; 67:1513–1520. [PubMed: 5274475]
4. Robison R. The possible significance of hexosephosphoric esters in ossification. Biochem J. 1923; 17:286–293. [PubMed: 16743183]
5. Meyer JL. Can biological calcification occur in the presence of pyrophosphate? Arch Biochem Biophys. 1984; 231:1–8. [PubMed: 6326671]
6. Rezende AA, Pizauro JM, Ciancaglini P, Leone FA. Phosphodiesterase activity is a novel property of alkaline phosphatase from osseous plate. Biochem J. 1994; 301:517–522. [PubMed: 8042997]
7. Hessle L, Johnsson KA, Anderson HC, et al. Tissue-nonspecific alkaline phosphatase and plasma cell membrane glycoprotein-1 are central antagonistic regulators of bone mineralization. Proc Natl Acad Sci USA. 2002; 99:9445–9449. [PubMed: 12082181]
8. Harmey D, Hessle L, Narisawa S, et al. Concerted regulation of inorganic pyrophosphate and osteopontin by Akp2, Enpp1, and Ank. Am J Pathol. 2004; 164:1199–1209. [PubMed: 15039209]
9. Terkeltaub RA. Inorganic pyrophosphate generation and disposition in pathophysiology. Am J Physiol Cell Physiol. 2001; 281:C1–C11. [PubMed: 11401820]
10. Huang R, Rosenbach M, Vaughn R, et al. Expression of the murine plasma cell nucleotide pyrophosphohydrolase PC-1 is shared by human liver, bone, and cartilage cells. Regulation of PC-1 expression in osteosarcoma cells by transforming growth factor-beta. J Clin Invest. 1994; 94:560–567. [PubMed: 8040311]
11. Johnson K, Moffa A, Chen Y, et al. Matrix vesicle plasma cell membrane glycoprotein-1 regulates mineralization by murine osteoblastic MC3T3 cells. J Bone Miner Res. 1999; 14:883–892. [PubMed: 10352096]
12. Gijsbers R, Ceulemans H, Stalmans W, Bollen M. Structural and catalytic similarities between nucleotide pyrophosphatases/phosphodiesterases and alkaline phosphatases. J Biol Chem. 2001; 276:1361–1368. [PubMed: 11027689]
13. Ciancaglini P, Yadav MC, Simão AMS, et al. Kinetic analysis of substrate utilization by native and TNAP-, NPP1-, or PHOSPHO1-deficient matrix vesicles. J Bone Miner Res. 2010; 25:716–723. [PubMed: 19874193]
14. Simão AMS, Yadav MC, Narisawa S, et al. Proteoliposomes harboring alkaline phosphatase and nucleotide pyrophosphatase as matrix vesicle biomimetics. J Biol Chem. 2010; 285:7598–7609. [PubMed: 20048161]
15. Ciancaglini P, Simão AMS, Camolezi FL, et al. Contribution of matrix vesicles and alkaline phosphatase to ectopic bone formation. Braz J Med Biol Res. 2006; 39:603–610. [PubMed: 16648897]
16. Ierardi DF, Pizauro JM, Ciancaglini P. Erythrocyte ghost cell-alkaline phosphatase: construction and characterization of a vesicular system for use in biomineralization studies. Biochim Biophys Acta. 2002; 1567:183–192. [PubMed: 12488052]
17. Ciancaglini P, Simão AMS, Bolean M, et al. Proteoliposomes in nanobiotechnology. Biophys Rev. 2012; 4:67–81.
18. Chakkalakal DA, Mashoof AA, Novak J, et al. Mineralization and pH relationships in healing skeletal defects grafted with demineralized bone matrix. J Biomed Mater Res. 1994; 28:1439–1443. [PubMed: 7876283]
19. Wu LNY, Genge BR, Dunkelberger DG, et al. Physicochemical characterization of the nucleational core of matrix vesicles. J Biol Chem. 1997; 272:4404–4411. [PubMed: 9020163]
20. Arnett TR. Acidosis, hypoxia and bone. Arch Biochem Biophys. 2010; 503:103–109. [PubMed: 20655868]
21. Bollen M, Gijsbers R, Ceulemans H, et al. Nucleotide pyrophosphatase/phophodiesterases on the move. Crit Rev Biochem Mol Biol. 2000; 35:393–432. [PubMed: 11202013]

22. Millán, JL. From biology to applications in medicine and biotechnology. Weinheim, Germany: Wiley-VCH Verlag GmbH & Co; 2006. Mammalian alkaline phosphatases.
23. Wu LN, Yoshimori T, Genge BR, et al. Characterization of the nucleational core complex responsible for mineral induction by growth plate cartilage matrix vesicles. J Biol Chem. 1993; 268:25084–25094. [PubMed: 8227072]
24. Wu LN, Genge BR, Dunkelberger DG, et al. Physicochemical characterization of the nucleational core of matrix vesicles. J Biol Chem. 1997; 272:4404–4411. [PubMed: 9020163]
25. Simão AMS, Beloti MM, Cezarino RM, et al. Membrane-bound alkaline phosphatase from ectopic mineralization and rat bone marrow cell culture. Comp Biochem Physiol A Mol Integr Physiol. 2007; 146:679–687. [PubMed: 16798036]
26. Gijsbers R, Ceulemans H, Bollen M. Functional characterization of the non-catalytic ectodomains of the nucleotide pyrophosphatase/phosphodiesterase NPP1. Biochem J. 2003; 371:321–330. [PubMed: 12533192]
27. Camolezi FL, Daghastanli KPR, Magalhães PP, et al. Construction of an alkaline phosphatase-liposome system: a tool for biomineralization study. Int J Biochem Cell Biol. 2002; 1282:1–11.
28. Hartree EF. Determination of protein: a modification of the Lowry method that gives a linear photometric response. Anal Biochem. 1972; 48:422–427. [PubMed: 4115981]
29. Pizauro JM, Ciancaglini P, Leone FA. Characterization of the phosphatidylinositol-specific phospholipase C-released form of rat osseous plate alkaline phosphatase and its possible significance on endochondral ossification. Mol Cell Biochem. 1995; 152:121–129. [PubMed: 8751158]
30. Heinonen JK, Lahti RJ. A new and convenient colorimetric determination of inorganic orthophosphate and its application to the assay of inorganic pyrophosphatase. Anal Biochem. 1981; 113:313–317. [PubMed: 6116463]
31. Leone FA, Baranauskas JA, Furriel RPM, et al. SigrafW: An easy-to-use program for fitting enzyme kinetic data. Biochem Molec Educ. 2005; 33:399–403.
32. Genge BR, Wu LN, Wuthier RE. Kinetic analysis of mineral formation during in vitro modeling of matrix vesicle mineralization: effect of annexin A5, phosphatidylserine, and type II collagen. Anal Biochem. 2007; 367:159–166. [PubMed: 17585866]
33. Wuthier RE, Rice GS, Wallace JE, et al. In vitro precipitation of calcium phosphate under intracellular conditions: Formation of brushite from an amorphous precursor in the absence of ATP. Calcif Tissue Int. 1985; 37:401–410. [PubMed: 3930038]
34. Wu LNY, Wuthier MG, Genge BR, et al. In situ levels of intracellular Ca^{2+} and pH in avian growth plate cartilage. Clin Orthop Relat Res. 1997; 335:310–324. [PubMed: 9020233]
35. Wuthier RE. Electrolytes of isolated epiphyseal chondrocytes, matrix vesicles, and extracellular fluid. Calcif Tissue Res. 1977; 23:125–133. [PubMed: 890549]
36. Genge BR, Wu LN, Wuthier RE. In vitro modeling of matrix vesicle nucleation: synergistic stimulation of mineral formation by annexin A5 and phosphatidylserine. J Biol Chem. 2007; 282:26035–26045. [PubMed: 17613532]
37. Boskey AL, Goldberg MR, Posner AS. Calcium-phospholipid-phosphate complexes in mineralizing tissue. Proc Soc Exp Biol Med. 1978; 157:590–593. [PubMed: 652797]
38. Wu LN, Genge BR, Sauer GR, Wuthier RE. Characterization and reconstitution of the nucleational complex responsible for mineral formation by growth plate cartilage matrix vesicles. Connect Tissue Res. 1996; 35:309–315. [PubMed: 9084669]
39. Termine JD, Peckauskas RA, Posner AS. Calcium phosphate formation in vitro: II. Effects of environment on amorphous crystalline transformation. Arch Biochem Biophys. 1970; 140:318–325. [PubMed: 4319593]
40. Eanes ED. Thermochemical studies on amorphous calcium phosphate. Calcif Tissue Res. 1970; 5:133–145. [PubMed: 5423622]
41. Wuthier RE, Lipscomb GF. Matrix vesicles: structure, composition, formation and function in calcification. Front Biosci. 2011; 16:2812–2902.
42. Wuthier RE. Lipids of mineralizing epiphyseal tissues in the bovine fetus. J Lipid Res. 1968; 9:68–78. [PubMed: 5637432]

43. Boskey AL, Posner AS. Extraction of a calcium-phospholipid-phosphate complex from bone. Calcif Tissue Res. 1976; 19:273–283. [PubMed: 3268]
44. Wuthier RE, Gore ST. Partition of inorganic ions and phospholipids in isolated cell, membrane and matrix vesicle fractions: evidence for Ca-Pi-acidic phospholipid complexes. Calcif Tissue Res. 1977; 24:163–171. [PubMed: 597754]
45. Valhmu WB, Wu LN, Wuthier RE. Effects of Ca/Pi ratio, Ca^{2+} × Pi ion product, and pH of incubation fluid on accumulation of $^{45}Ca^{2+}$ by matrix vesicles in vitro. Bone Miner. 1990; 8:195–209. [PubMed: 2157511]
46. Wu LN, Genge BR, Wuthier RE. Analysis and molecular modeling of the formation, structure, and activity of the phosphatidylserine-calcium-phosphate complex associated with biomineralization. J Biol Chem. 2008; 283:3827–3838. [PubMed: 18077457]
47. Bennett RM, Lehr JR, McCarty DJ. Factors affecting the solubility of calcium pyrophosphate dihydrate crystals. J Clin Invest. 1975; 56:1571–1579. [PubMed: 423]
48. Prasad, R. Manual of membrane lipids. Berli Heidelderg: Springer-Verlag; 1996.
49. Simão AMS, Yadav MC, Ciancaglini P, Millán JL. Proteoliposomes as matrix vesicles' biomimetics to study the initiation of skeletal mineralization. Braz J Med Biol Res. 2010; 43:234–241. [PubMed: 20401430]
50. Roberts S, Narisawa S, Harmey D, et al. Functional involvement of PHOSPHO1 in matrix vesicle-mediated skeletal mineralization. J Bone Miner Res. 2007; 22:617–627. [PubMed: 17227223]
51. Xiao Z, Camalier CE, Nagashima K, et al. Analysis of the extracellular matrix vesicle proteome in mineralizing osteoblasts. J Cell Physiol. 2007; 210:325–335. [PubMed: 17096383]
52. Eanes ED. Biophysical aspects of lipid interaction with mineral: liposome model studies. Anat Rec. 1989; 224:220–225. [PubMed: 2672886]
53. Carruthers A, Melchior DL. How bilayer lipids affect membrane protein activity. TIBS. 1986; 11:331–335.
54. Anderson HC, Hsu HH, Morris DC, et al. Matrix vesicles in osteomalacic hypophosphatasia bone contain apatite-like mineral crystals. Am J Pathol. 1997; 151:1555–1561. [PubMed: 9403706]
55. Wu LN, Genge BR, Kang MW, et al. Changes in phospholipid extractability and composition accompany mineralization of chicken growth plate cartilage matrix vesicles. J Biol Chem. 2002; 277:5126–5133. [PubMed: 11714705]
56. Lehto MT, Sharom FJ. Release of the glycosylphosphatidylinositol-anchored enzyme ecto-5'-nucleotidase by phospholipase C: catalytic activation and modulation by the lipid bilayer. Biochem J. 1998; 332:101–109. [PubMed: 9576857]
57. Lehto MT, Sharom FJ. Proximity of the protein moiety of a GPI-anchored protein to the membrane surface: a FRET study. Biochemistry. 2002; 41:8368–8376. [PubMed: 12081485]
58. Lazic S. Microcrystalline hydroxyapatite formation from alkaline solutions. J Crystal Growth. 1995; 147:147–154.
59. Guicheux J, Palmer G, Shukunami C, et al. A novel in vitro culture system for analysis of functional role of phosphate transport in endochondral ossification. Bone. 2000; 27:69–74. [PubMed: 10865211]
60. Wu LN, Sauer GR, Genge BR, et al. Effects of analogues of inorganic phosphate and sodium ion on mineralization of matrix vesicles isolated from growth plate cartilage of normal rapidly growing chickens. J Inorg Biochem. 2003; 94:221–235. [PubMed: 12628702]
61. Balcerzak M, Malinowska A, Thouverey C, et al. Proteome analysis of matrix vesicles isolated from femurs of chicken embryo. Proteomics. 2008; 8:192–205. [PubMed: 18095356]
62. Hsu HH, Camacho NP, Anderson HC. Further characterization of ATP-initiated calcification by matrix vesicles isolated from rachitic rat cartilage. Membrane perturbation by detergents and deposition of calcium pyrophosphate by rachitic matrix vesicles. Biochim Biophys Acta. 1999; 1416:320–332. [PubMed: 9889389]

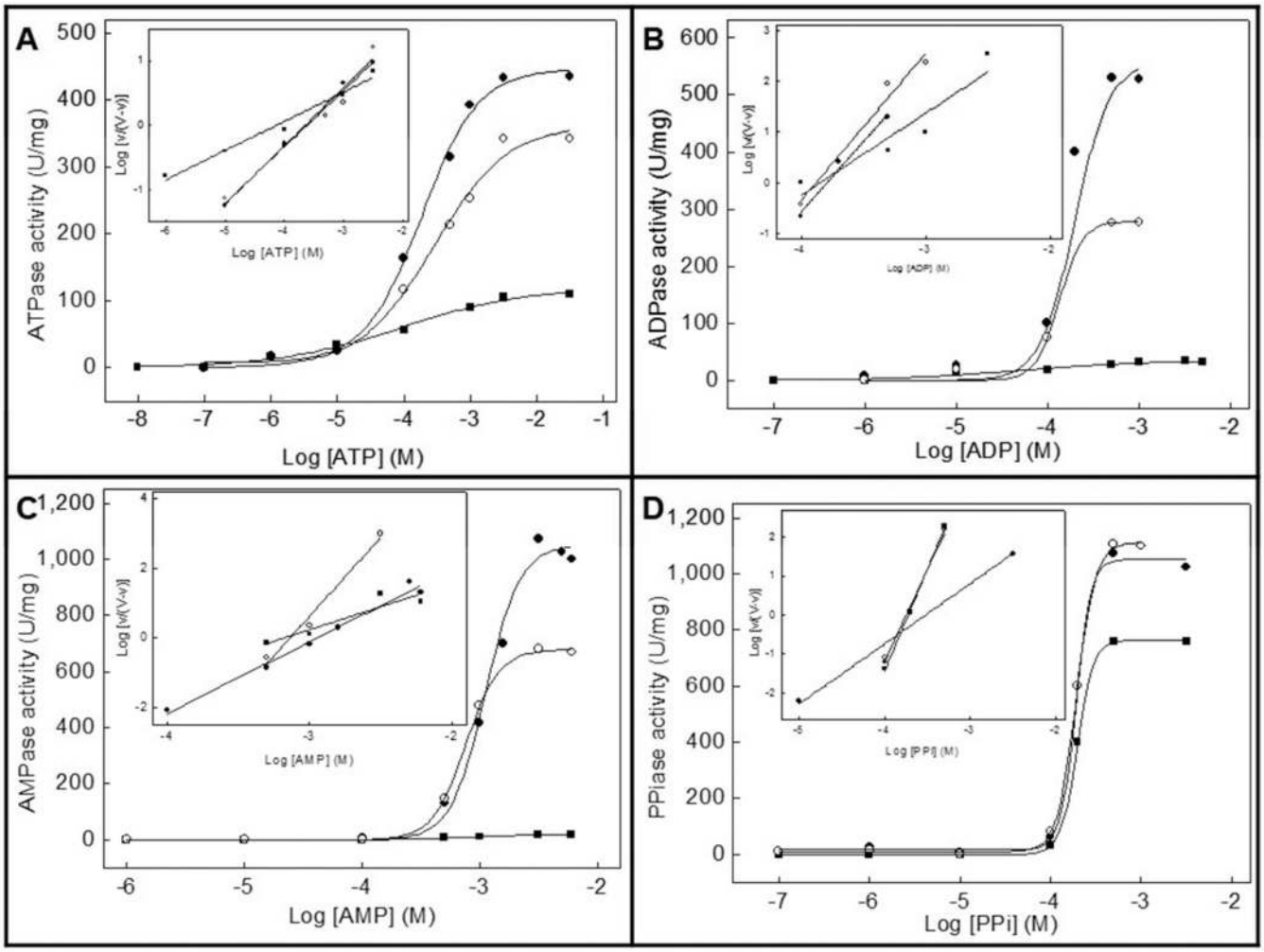

Fig 1.

Effect of increasing concentrations of **(a)** ATP, **(b)** ADP, **(c)** AMP and **(d)** PP_i on the P_i-generating activity of DPPC proteoliposomes containing: (●) TNAP, (■) NPP1 or (○) TNAP plus NPP1. Assays were done at 37 °C and buffered with 50 mM AMPOL, pH 8, containing 2 mM $MgCl_2$ and substrate and released P_i measured

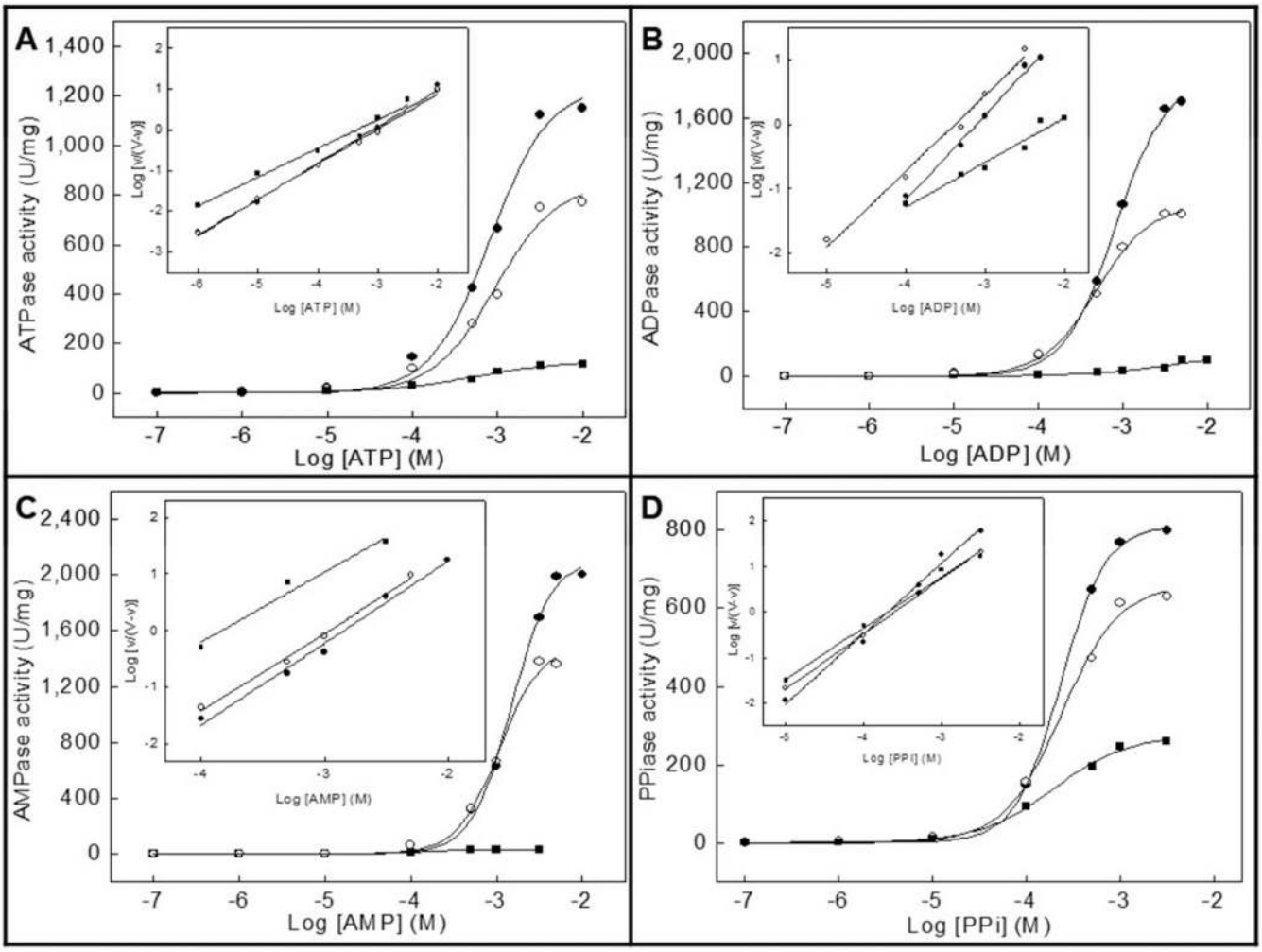

Fig 2.

Effect of increasing concentrations of **(a)** ATP, **(b)** ADP, **(c)** AMP and **(d)** PP_i on the P_i-generating activity of DPPC proteoliposomes containing: (●) TNAP, (■) NPP1 or (○) TNAP plus NPP1. Assays were done at 37 °C and buffered with 50 mM AMPOL, pH 9, containing 2 mM $MgCl_2$ and substrate and released P_i measured

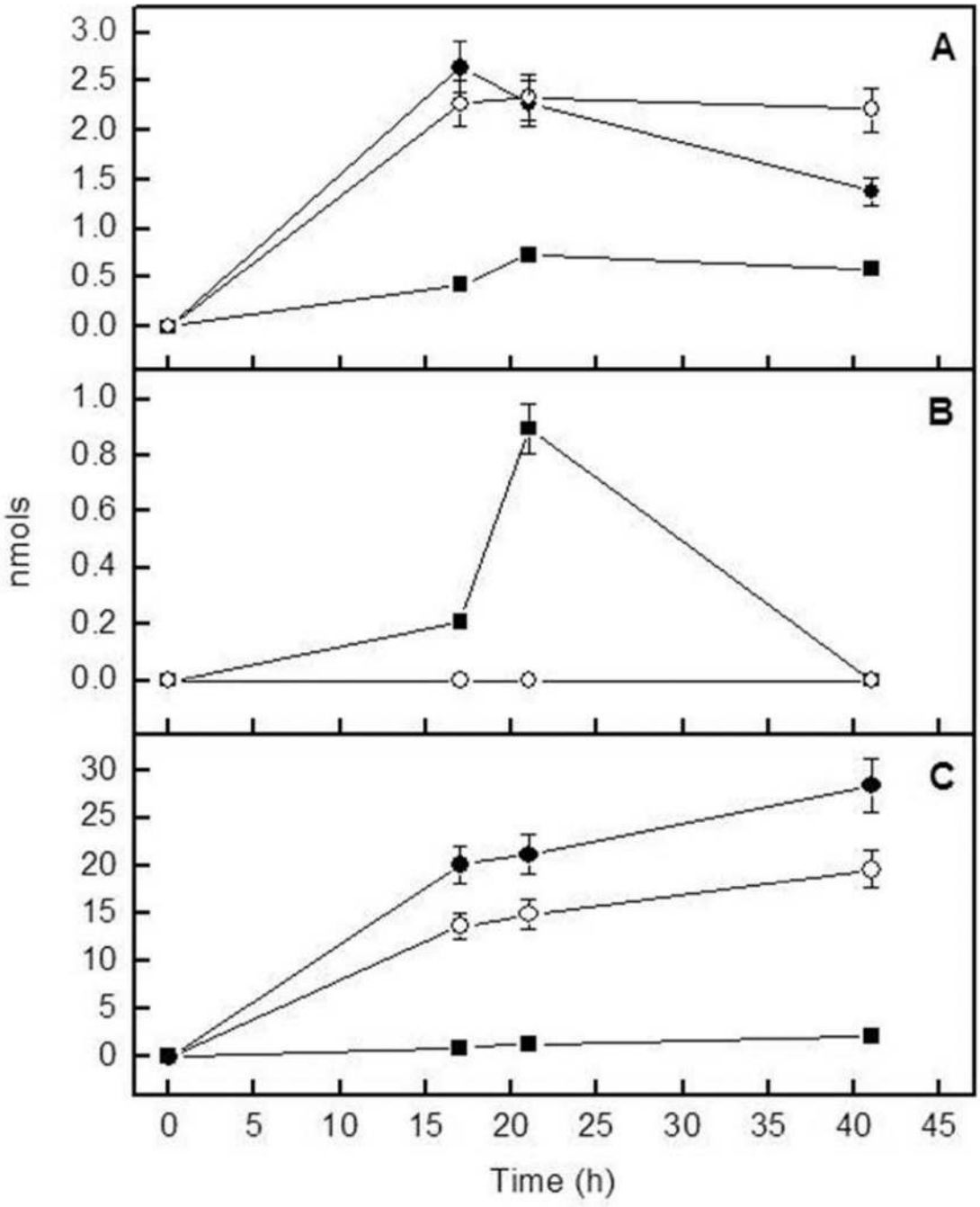

Fig 3.

Progression of the formation of **(a)** ADP, **(b)** AMP and **(c)** adenosine during hydrolysis of 100 nmol of ATP by (●) TNAP-proteoliposomes, (■) NPP1-proteoliposomes and (■) TNAP plus NPP1-proteoliposomes. Hydrolysis was determined in 50 mM AMPOL buffer, pH 9, containing 2 mM $MgCl_2$ and 1 mM ATP. Nucleotide concentrations were monitored by HPLC

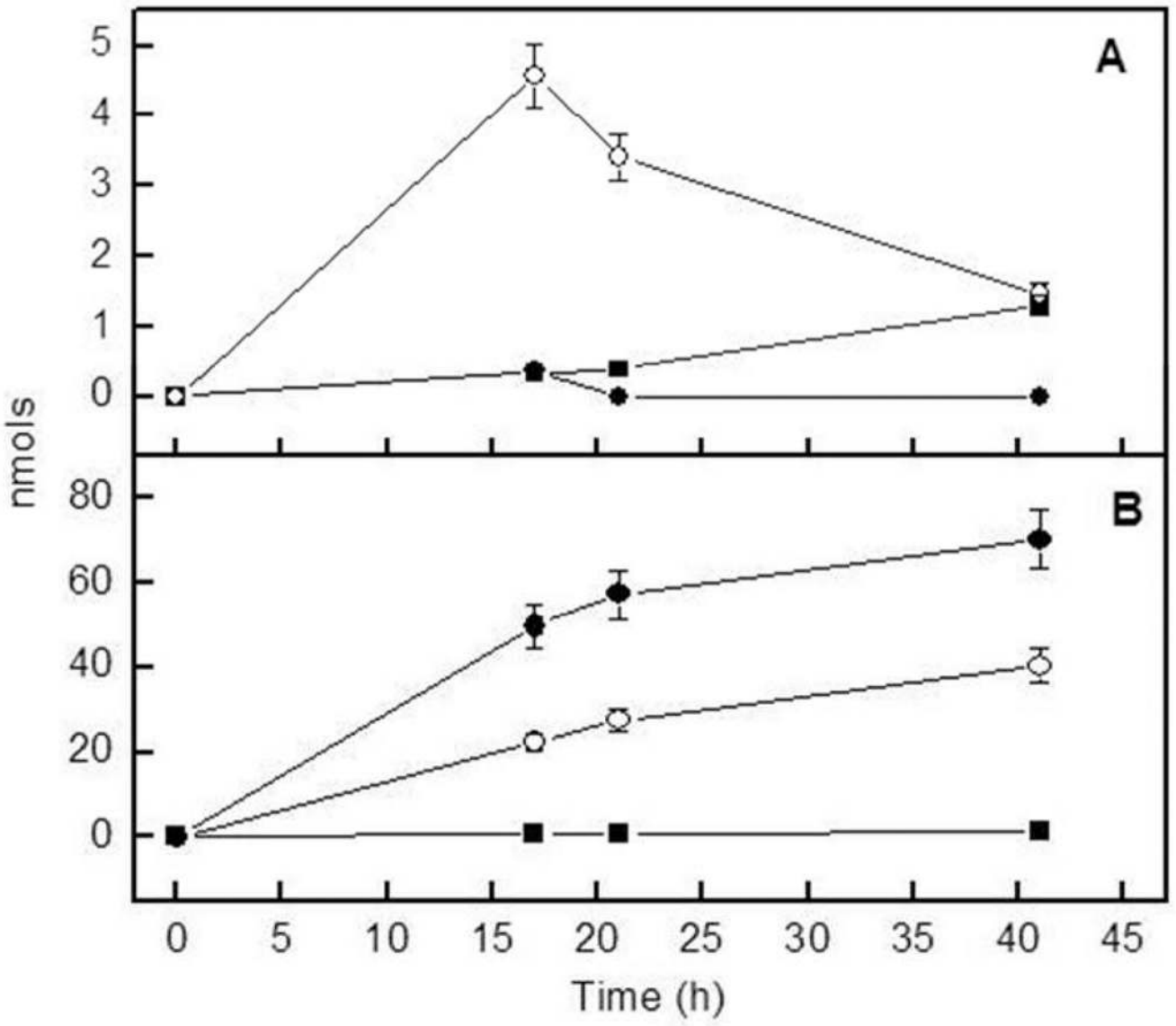

Fig 4.

Progression of the formation of **(a)** AMP and **(b)** adenosine during hydrolysis of 100 nmol of ADP by (●) TNAP-proteoliposomes, (■) NPP1-proteoliposomes and (○) TNAP plus NPP1-proteoliposomes. Hydrolysis was determined in 50 mM AMPOL buffer, pH 9, containing 2 mM $MgCl_2$ and 1 mM ADP. Nucleotide concentrations were monitored by HPLC

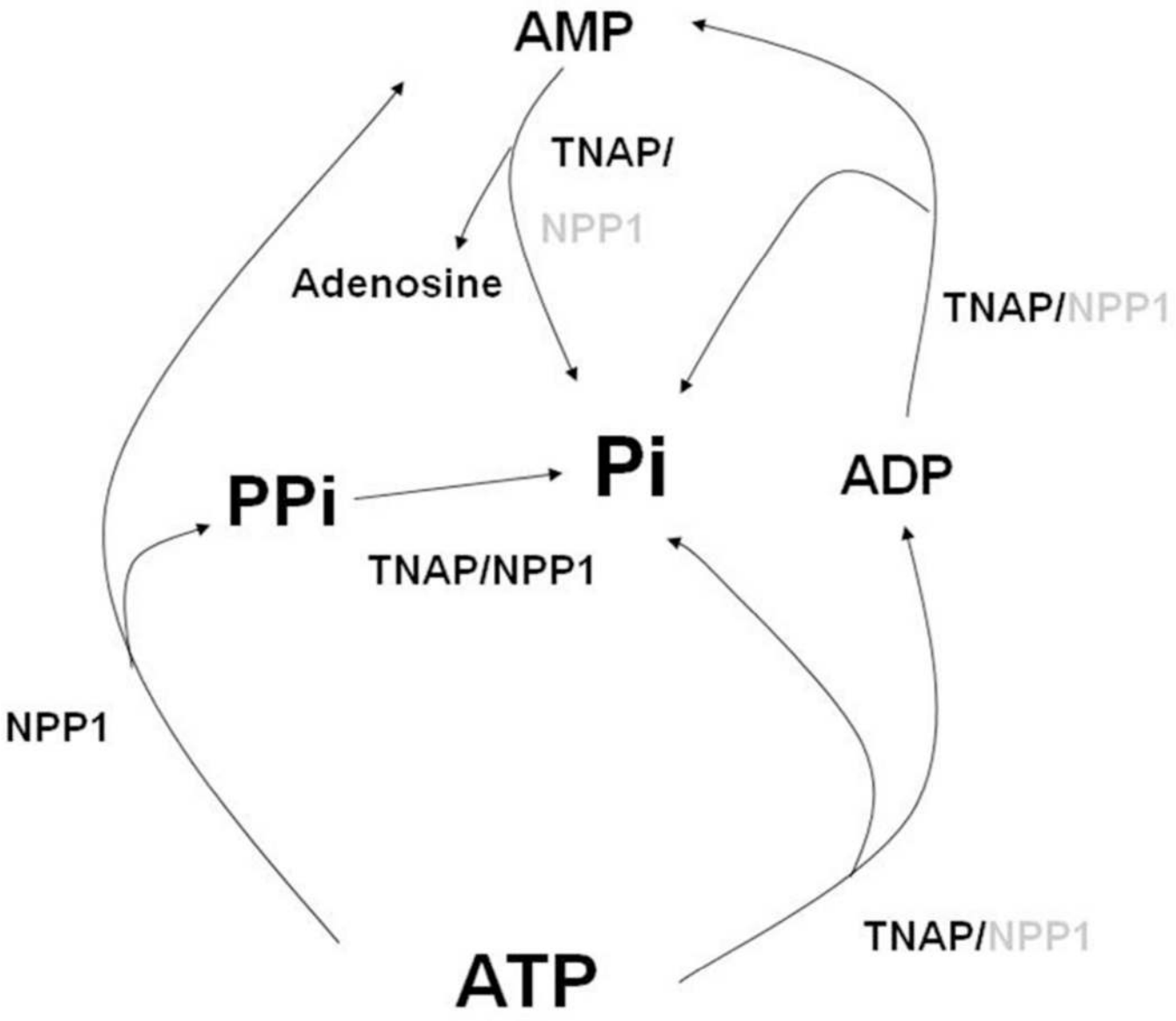

Fig 5.

Representation of all the possible simultaneous enzymatic reactions during catalysis of substrates by TNAP and NPP1 at alkaline pH. Indicated in black and gray are the enzymes with higher and lower catalytic efficiencies, respectively, for the indicated substrates

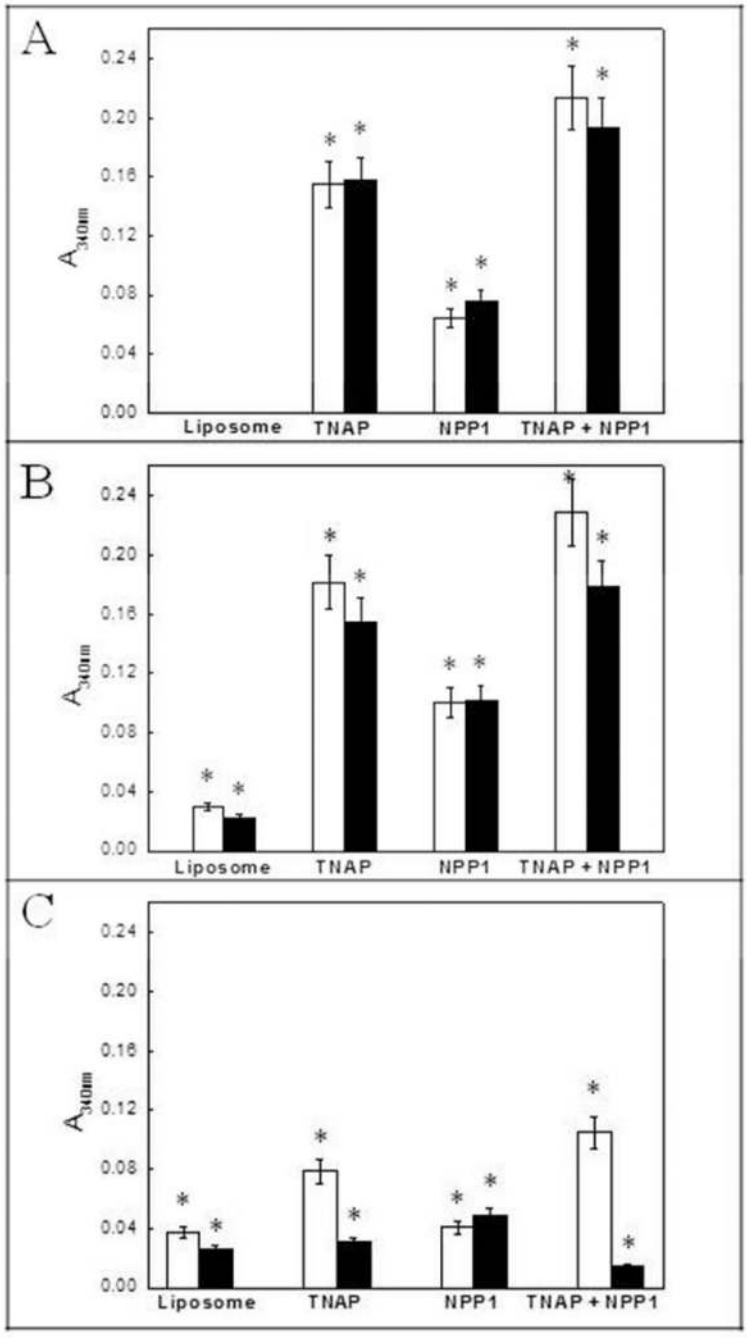

Fig 6.

Effect of TNAP-, NPP1-, and TNAP plus NPP1-proteoliposomes on mineralization of ACP and PS-CPLX-seeded SCL, at pH 7.5 **(A)**, 8 **(B)** and 9 **(C)**, in the presence of 1 mM ATP, after 48 h of incubation at 37°C. White bars: PS-CPLX-seeded SCL. Black bars: ACP-seeded SCL. The ACP and PS-CPLX nucleators were prepared and mineralization was monitored in the microplate, as described in Materials and Methods. Empty liposomes without incorporated enzymes were used as control, and the bars show the increment in absorbencies over 48h.

Table 1

Kinetic parameters for the hydrolysis of substrates by TNAP-, NPP1-, or TNAP + NPP1-proteoliposomes. Kinetic analysis was performed in 50 mM Tris-HCl buffer, pH 8, containing 2 mM $MgCl_2$ and substrate.

Substrates	Kinetic parameters	Proteoliposomes		
		TNAP	NPP1	TNAP + NPP1
ATP	V_m (U/mg)	446 ± 37	120 ± 15	363 ± 24
	$K_{0.5}$ (mM)	0.19 ± 0.01	0.095 ± 0.01	0.28 ± 0.02
	n	0.90 ± 0.07	0.45 ± 0.03	0.87 ± 0.05
	$k_{cat}/K_{0.5}$ ($M^{-1}.s^{-1}$)	4,522	2,741	-
PP_i	V_m (U/mg)	1,053 ± 83	765 ± 41	1,113 ± 98
	$K_{0.5}$ (mM)	0.19 ± 0.01	0.20 ± 0.008	0.19 ± 0.007
	n	1.5 ± 0.08	5.2 ± 0.4	4.7 ± 0.3
	$k_{cat}/K_{0.5}$ ($M^{-1}.s^{-1}$)	11,084	8,300	-
ADP	V_m (U/mg)	558 ± 42	35 ± 2.8	279 ± 20
	$K_{0.5}$ (mM)	0.20 ± 0.02	0.053 ± 0.004	0.13 ± 0.01
	n	2.8 ± 0.1	1.6 ± 0.09	2.9 ± 0.2
	$k_{cat}/K_{0.5}$ ($M^{-1}.s^{-1}$)	5,580	1,433	-
AMP	V_m (U/mg)	1,051 ± 73	19 ± 1.7	680 ± 43
	$K_{0.5}$ (mM)	1.1 ± 0.08	0.71 ± 0.05	0.76 ± 0.03
	n	2.0 ± 0.1	4.2 ± 0.2	4.5 ± 0.3
	$k_{cat}/K_{0.5}$ ($M^{-1}.s^{-1}$)	1,911	58	-

Table 2

Kinetic parameters for the hydrolysis of substrates by TNAP-, NPP1-, or TNAP + NPP1-proteoliposomes. Kinetic analysis was performed in 50 mM AMPOL buffer, pH 9, containing 2 mM $MgCl_2$ and substrate.

Substrates	Kinetic parameters	Proteoliposomes		
		TNAP	NPP1	TNAP + NPP1
ATP	V_m (U/mg)	1,243 ± 37	131 ± 10	849 ± 73
	$K_{0.5}$ (mM)	0.82 ± 0.07	0.54 ± 0.04	0.93 ± 0.08
	n	0.90 ± 0.05	0.71 ± 0.02	0.86 ± 0.05
	$k_{cat}/K_{0.5}$ ($M^{-1}.s^{-1}$)	3,033	526	-
PP_i	V_m (U/mg)	813 ± 61	276 ± 15	660 ± 58
	$K_{0.5}$ (mM)	0.23 ± 0.02	0.19 ± 0.02	0.24 ± 0.03
	n	1.5 ± 0.07	1.1 ± 0.01	1.2 ± 0.08
	$k_{cat}/K_{0.5}$ ($M^{-1}.s^{-1}$)	7,066	3,151	-
ADP	V_m (U/mg)	1,856 ± 95	179 ± 20	1,069 ± 97
	$K_{0.5}$ (mM)	0.82 ± 0.06	6.7 ± 0.14	0.49 ± 0.04
	n	1.3 ± 0.04	0.69 ± 0.02	1.2 ± 0.03
	$k_{cat}/K_{0.5}$ ($M^{-1}.s^{-1}$)	4,527	58	-
AMP	V_m (U/mg)	2,114 ± 84	30 ± 2.7	1,503 ± 140
	$K_{0.5}$ (mM)	1.5 ± 0.2	0.15 ± 0.01	1.1 ± 0.2
	n	1.4 ± 0.09	1.2 ± 0.03	1.4 ± 0.06
	$k_{cat}/K_{0.5}$ ($M^{-1}.s^{-1}$)	2,818	435	-

Table 3

Comparison between the kinetic parameters obtained at different pHs for the hydrolysis of the indicated substrates by DPPC proteoliposomes containing TNAP, NPP1 or TNAP + NPP1.

Substrate	Kinetic parameters	pH 8.0/ pH 7.4[a] Ratios for Proteoliposomes			pH 9.0/ pH 7.4[a] Ratios for Proteoliposomes		
		TNAP	NPP1	TNAP + NPP1	TNAP	NPP1	TNAP + NPP1
ATP	V_m	27	36	24	76	39	56
	$K_{0.5}$	1.6	5.9	1.8	6.8	34	5.8
	$k_{cat}/K_{0.5}$	12	6.1	-	7.9	1.2	-
PP_i	V_m	37	209	80	29	75	47
	$K_{0.5}$	0.27	2.9	1.0	0.32	2.7	1.3
	k_{cat}/K0.5	29	73	-	18	28	-
ADP	V_m	25	7.2	20	83	37	76
	$K_{0.5}$	0.71	0.74	0.87	2.9	93	3.3
	$k_{cat}/K_{0.5}$	27	9.7	-	22	0.4	-
AMP	V_m	45	4.0	41	90	6.3	91
	$K_{0.5}$	1.5	3.6	1.5	2.1	0.75	2.2
	$k_{cat}/K_{0.5}$	0.31	1.1	-	0.46	8.5	-

[a]Data at pH 7.4 are described in [14].